SUPPLEMENTARY INFORMATION for

# Modulation of Molecular Hybridization and Charge Screening in a Carbon Nanotube Channel using the Electrical Pulse Method

*Jun-Myung Woo,*[a, *] *Seok Hyang Kim,*[a, *] *Honnggu Chun,*[b] *Sung Jae Kim,*[a, c]

*Jinhong Ahn,*[a] *and Young June Park.*[a, †]

[a] Department of Electrical and Computer Engineering, Seoul National University, Seoul 151-744, Republic of Korea.

[b] Department of Biomedical Engineering, Korea University, Horimkwan 116, Seoul 136-703, Republic of Korea.

[c] Inter-university Semiconductor Research Center, Seoul National University, Seoul 151-744, Republic of Korea.

[†] CORRESPONDING AUTHOR: Young June Park (ypark@snu.ac.kr)

**1. The ohmic contact between the Au electrode and CNT**

We have employed an Au electrode, which has a large work function (~ 5.1eV) as shown in Figure S1 (a), for an improvement of the contact property. Figure S1 (c) shows the typical *I-V* characteristics of a CNN device, with the Au electrode system shown in Figure S1 (b). This result leads to a conclusion that the contact between the Au electrode and the CNT is an Ohmic contact. If one uses a low work function material, such as Al, the $R_{contact}$ in Figure S1 (b) should be carefully considered.

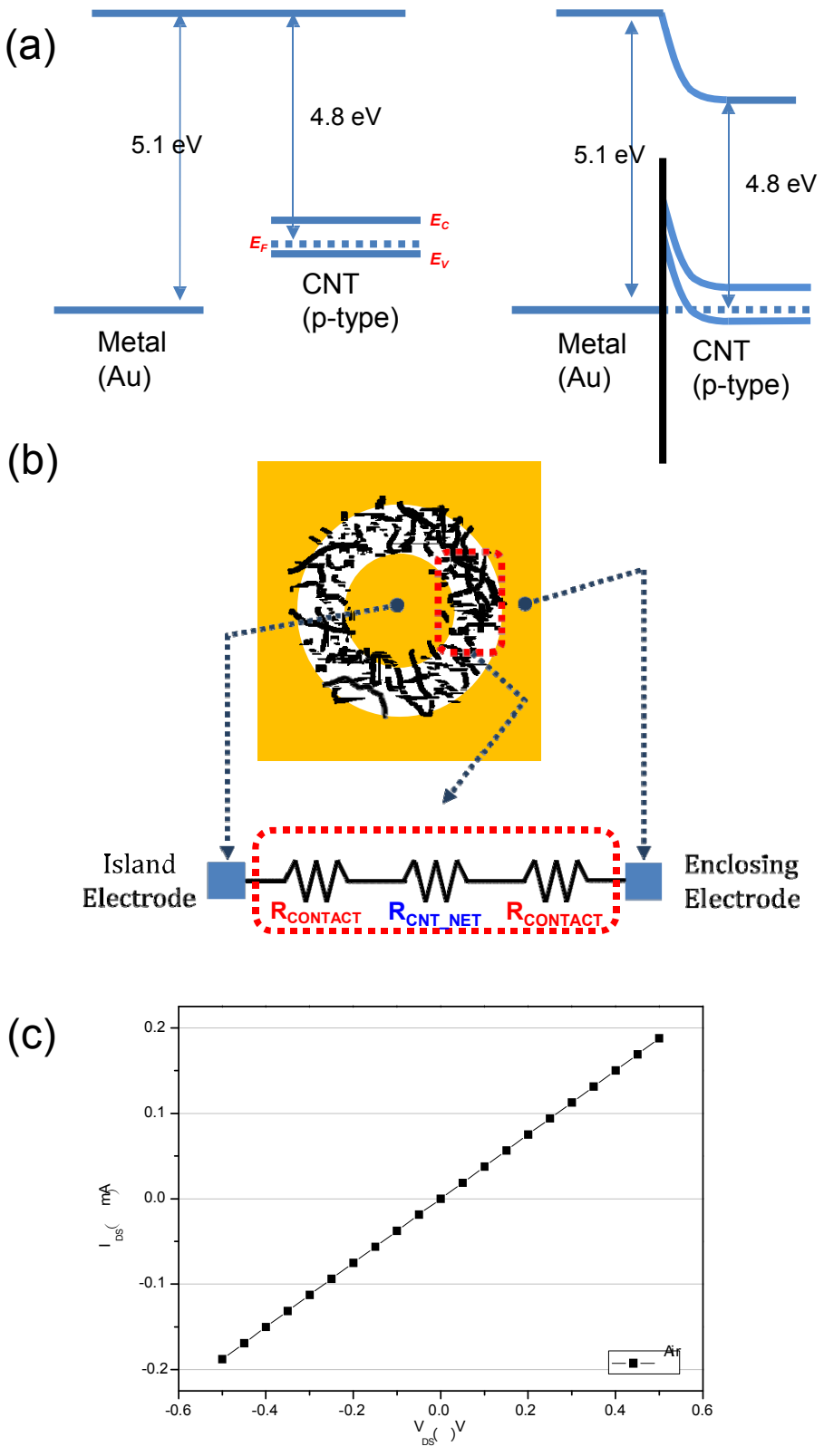


Figure S1. (a) Suggested band diagram of the device. The CNT with a work function of ~4.8 eV is connected to an Au electrode. Owing to the difference in work function between the CNT and the Au,

ohmic contact can be obtained. (b) Conceptual scheme of the CNN channel between the island electrode and enclosing electrode. (c) The *I-V* curve was taken with the voltage applied to drain from -0.5 V to +0.5 V, and the source is 0 V. The conductance through electrode-CNT leads to ohmic behavior.

**2. Simulation result of surface charge redistribution due to pulse bias**

The electrical potential and charged carriers in the electrolyte solution are governed by the Poisson equation,

$$\nabla \cdot \varepsilon(-\nabla\psi) = q([n^+]-[n^-]), \tag{S1}$$

where, $\varepsilon$ is the permittivity of electrolyte solution, $\psi$ is the electrical potential, and $[n^+]$ and $[n^-]$ are the density number of the cation and anion in the electrolyte solution, respectively.

In the electrolyte solutions, ion carriers accelerate through the drift and diffusion, similar to the transport of electrons and holes in the semiconductor. Accordingly, the ion flux is represented by

$$F_{[n^\pm]} = \pm\mu_{n^\pm}[n^\pm]\nabla\psi - D_{n^\pm}\nabla[n^\pm], \tag{S2}$$

where, $\mu_{n\pm}$ and $D_{n\pm}$ are the mobility and the diffusion coefficient of cation and anion, respectively, in the electrolyte solution.

The continuity equation for ion carriers can be written as

$$\frac{\partial[n^\pm]}{\partial t} = -\nabla \cdot F_{[n^\pm]}. \tag{S3}$$

In the steady state, the left term of Eq. S3 becomes zero, yielding the Boltzmann distribution for ions,

$$[n^\pm] = n_0 \exp(\mp\psi / V_t), \tag{S4}$$

where, $n_0$ is the bulk ion concentration of the electrolyte solution. The diffuse layer derives from this distribution, suggested by Gouy and Chapman.

After Stern's modification that considers the Helmholtz layer due to the minimum distance between the ions and the electrode surface, the EDL has been regarded as a series capacitance, made up of the Helmholtz layer and diffuse layer.

The parameters and simulation conditions used in this work are summarized in Table S2 and Figure S2. The electrical potential $\psi_0$ is applied to the electrode, with respect to the bulk solution, which is grounded by the reference electrode. Generally, semiconductors are employed as the electrode in affinity-based biosensors, to detect the charge induced by charged molecules. The electrode surface charge induced by charged molecules is calculated from

$$Q = -\int \mathbf{D} \cdot d\mathbf{s} \,. \tag{S5}$$

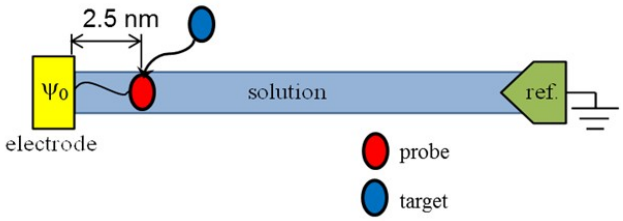


Figure S2. Schematic diagram of the probe-target binding event in the affinity-based biosensor.

| Parameter | Value | Note |
|---|---|---|
| $\varepsilon$ | 78 * $\varepsilon_0$ | aqueous solution in room temperature |
| $\mu_{H+}$ | 33.3 * $10^{-4}$ $cm^2$/V-s | |
| $\mu_{OH-}$ | 18.8 * $10^{-4}$ $cm^2$/V-s | |
| $\mu_{Na+}$ | 5.9 * $10^{-4}$ $cm^2$/V-s | |
| $\mu_{Cl-}$ | 7.0 * $10^{-4}$ $cm^2$/V-s | |
| $D_{n\pm}$ | $\mu k_B T/q$ | Einstein relation |
| $n_0$ | 0.1 M | in buffer solution |
| $d_H$ | 5 Å | thickness of Helmholtz layer |

Table S1. Parameters used in this simulation

Figure S3 shows the change of the induced charge variation, and the sensitivity, with time. At $t$ = 0 sec, step pulse voltage is applied to the electrode (distance = 0), in the buffer condition. High step pulse bias induces the electro-diffusion flow of mobile ions on the transient state, so that the screening length

is instantaneously extended. As the screening length is extended, the sensitivity increases to reach the maximum, and decreases again, as the system settles down at the steady state.

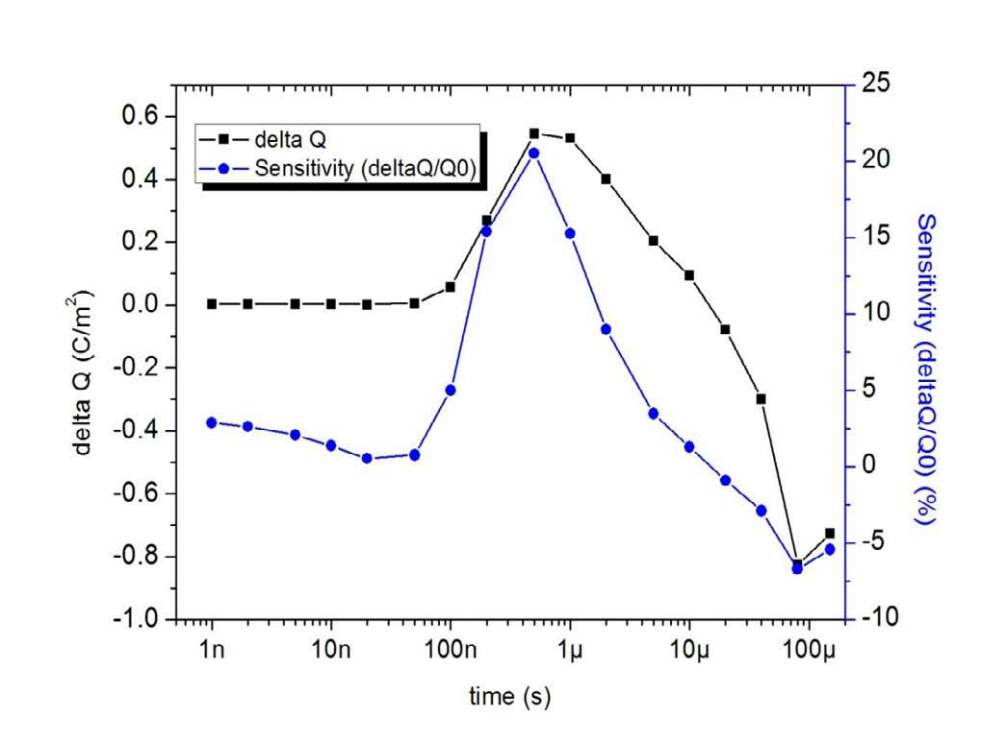


Figure S3. Variance of induced surface charge and corresponding sensitivity with respect to time, after step-pulse biasing in the buffer solution.

### 3. Details of the self-gating effect

Figures S4 (a) and (b) show the schematics diagram of the bare CNN device and its equivalent circuit, which is basically a two-terminal resistor, with the electrolyte droplet as the gate. While the electrolyte gate is floated, however, it is capacitively coupled with the island electrode (drain) and enclosing electrode (source). The electrostatic potential of the electrolyte follows the potential of the source, as the source-electrolyte capacitance is much larger than the drain-electrolyte capacitance ($C_S >> C_D$). Notice that the butting area between the electrolyte and source is much larger, than that between the electrolyte and drain. The source electrode is shared with other devices.

The unique asymmetric feature of the two electrodes system is manifested as the asymmetric current versus voltage *(I-V)* characteristics between the two electrodes. We have previously reported this *"self gating effect"* using a unique biosensor architecture, consisting of two gold electrodes with concentric structures (Kim et al., *Appl. Phys. Lett,* 2008, **93**, 243115(1-3)). Figure S4 (c) shows the *I-V* characteristics of a representative bare CNN device, in which the drain voltage is swept from –0.5 V ~ to +0.5 V, while the source voltage is fixed at 0 V. Due to the aforementioned *self gating effect*, the measured current shows the well known asymmetric behavior, with respect to the polarity of the $V_{DS}$. This is the diode characteristic for positive $V_{DS}$, and the saturation pMOSFET characteristic for negative $V_{DS}$. Notice here that our CNN channel is a p-type semiconductor, with positive threshold voltage.

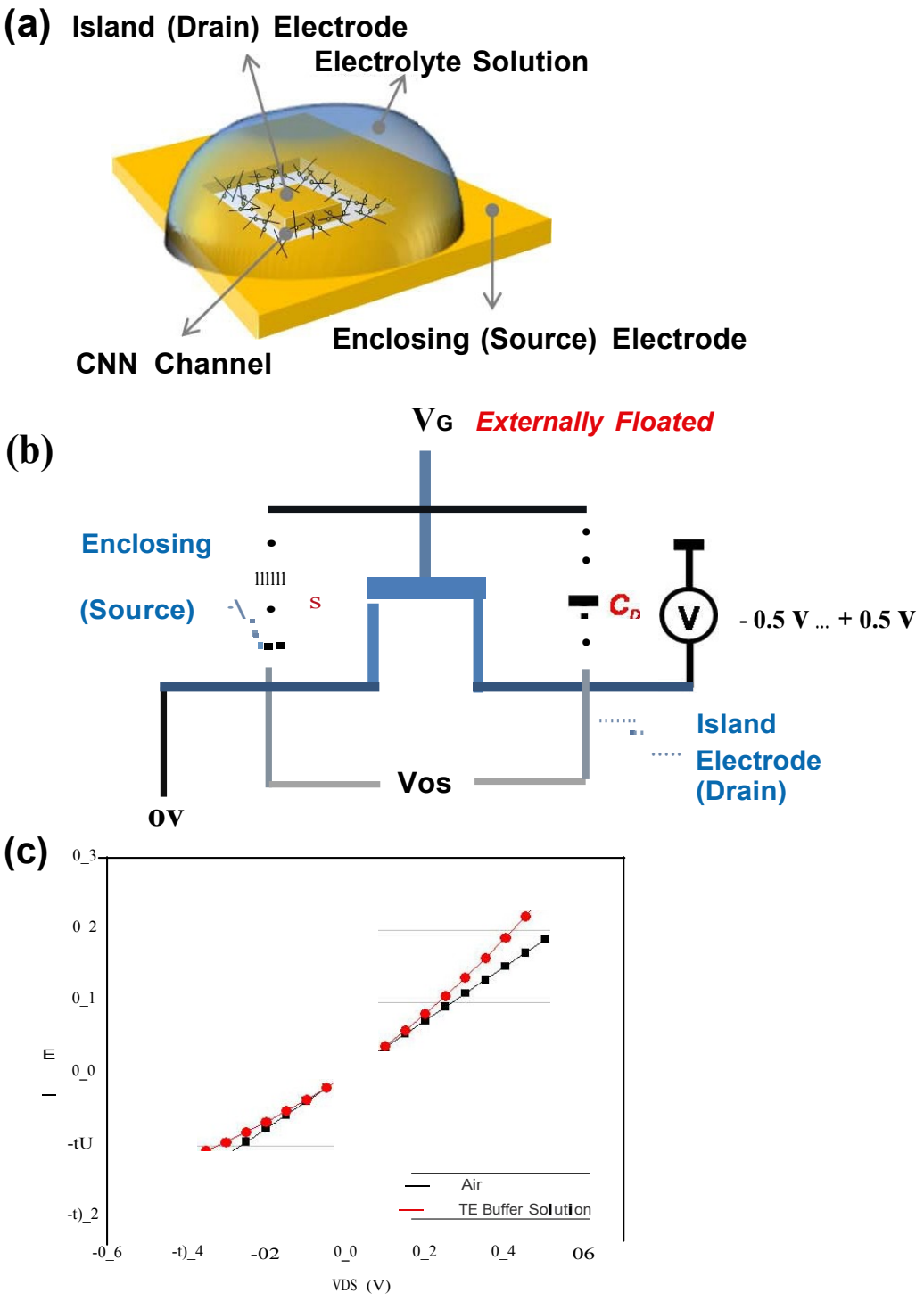


Figure S4. (a) The schematics of the concentric structure. (b) The equivalent circuit diagram of the concentric structure, which has two electrodes. (c) The current versus voltage characteristics of a CNN fabricated on the concentric structure with the floated gate.

**4. Sensing mechanism in terms of Au work function**

It is known that hybridization of target-DNA to the probe-DNA on the Au electrode results in a local change in the Au work function as schematically shown in Figure S5 (Sumi et al., Electroanal. Chem, 2003, 550, 321-325, Cui et al., Nano letters, 2003, 3, 783-787, Appenzeller et al., Phys. Rev. Lett, 2002, 89, 126801, Chen et al., Journal of the American Chemical Society, 2004, 126, 1563-1568). The DNA immobilization of p-DNA and hybridization with t-DNA on the Au electrode reduce the Au work function and increase the Schottky barrier, thereby increasing the contact resistance and leading to a decreasing the conductance of the devices (Ko et al., ACS Nano, 2011, 5, 4365-4372).

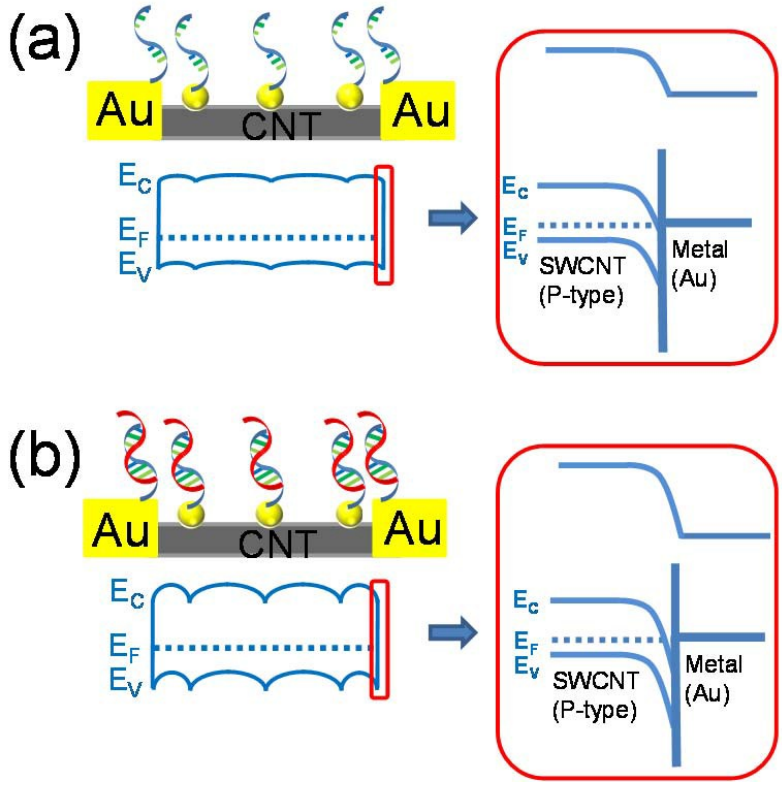


Figure S5. Schematics and corresponding energy band diagram of the device. The work function of Au is decreased by DNA hybridization. (a) The Schottky barrier increases and the hole carriers are depleted. (b) The conductance through CNT decreases due to the reduction of Au work function. ($E_C$ (Conduction band) : An energy band in which electrons can move freely in a solid, producing net transport of charge, $E_V$ (Valence band) : The highest electronic energy band in a semiconductor which can be filled with

electrons, EF (Fermi level) : The energy level at which the Fermi-Dirac distribution function of an assembly offermions is equal to one-half.)

**5. Simulation result of the time constant for transient measurements**

The redistribution of the EDL ion is related to the RC constants of the whole system consisting of the electrode, electrolyte and CNN channel, so that the whole system should be considered, to estimate the time response. Figure S6 (a) shows the equivalent circuit, which consists of pMOSFET, $R_i$, $C_i$, representing the CNT network, resistances of the electrolyte solution, and the capacitances of EDL, respectively.

Each parameter used in the equivalent circuit is described by the following equations.

$$R_i = \rho_{buffer} \frac{l_i}{s_i}, \tag{S6}$$

where, $R_i$ is the Buffer solution (NaCl concentration of 100mM) resistance ($i$ = D, G, S), $\rho_{buffer}$ (1.067 ohm·m) is the Buffer solution resistivity, $l_i$ is the distance between the top of the electrolyte droplet and each node in the electrode and channel, and $s_i$ is the cross-sectional area of each node. The EDL capacitance per unit area, $C_0$ is expressed as

$$C_0 = \sqrt{\frac{2n_0 \varepsilon\varepsilon_0 z^2 e^2}{kT} \cosh\left(\frac{ze\varphi_0}{2kT}\right)}, \tag{S7}$$

where, $\varepsilon\varepsilon_0$ is the DI water permittivity, $n_0$ is the number density of the ionic species (NaCl : 100 mM), and $\hat{}_{\square}$ is the electric surface potential. Since the surface area of the source electrode is much greater than the surface area of the drain electrode, we set $C_S \approx 1000 C_D$, under the assumption that the area of the source electrode is 1000 times larger than the drain electrode area.

The results from the equivalent circuit were validated using the $I_{DS}$-$V_{DS}$ curve with experimental measurements, as shown in Figure S6 (b). Figure S6 (c) shows the transient measurement results for experiment and simulation in the PBS buffered solution. The time duration for the initial transient behavior is defined by the time constant, $\tau_{RC}$, and it can be estimated as ~ O(1) micro-seconds, under the

assumption that the PBS buffered solution contains NaCl (100mM). Experimental data show slightly incremental behavior after $\tau_{RC}$, but the transient current should be measured within $\tau_{RC}$, so that the increasing time part may be neglected.

When a pulse bias is applied to the sensor system that includes an electrolyte solution, ions forming EDL are redistributed, according to the applied bias condition. The time required to reach the steady state is determined by $\tau_{RC}$, which is related to the mobility, and the concentration of the ions within the electrolyte solution (Woo et al., *IEEE SISPAD,* 2012, 177-180). The mobility of the ions in the electrolyte solution is significantly lower than that of the electrons and holes in the semiconductor, thus the $\tau_{RC}$ of the sensor system is large enough to perform the transient electrical measurements.

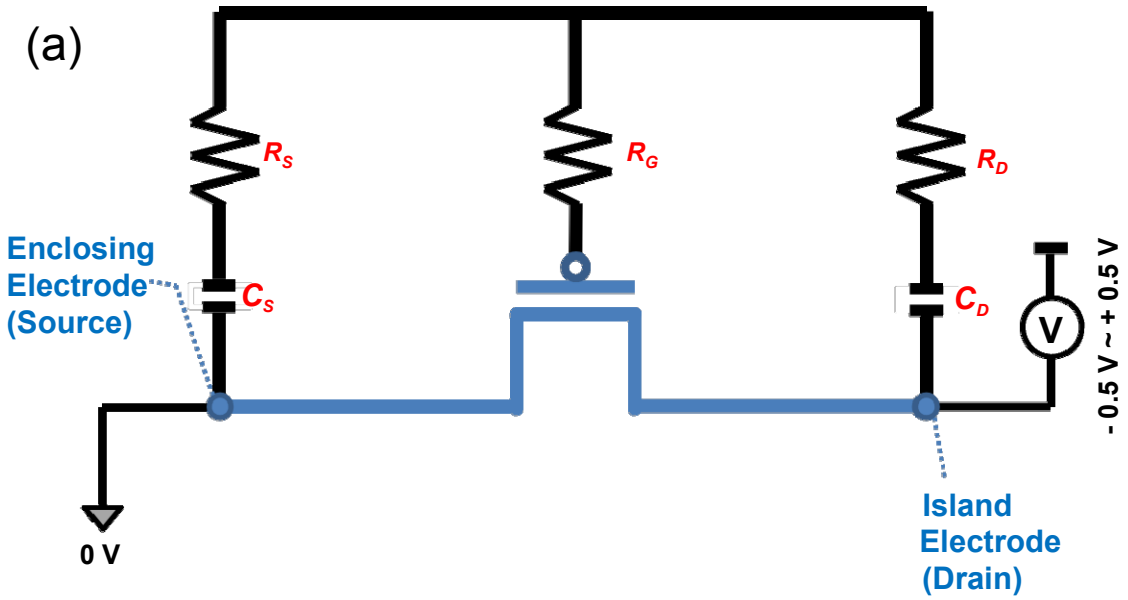

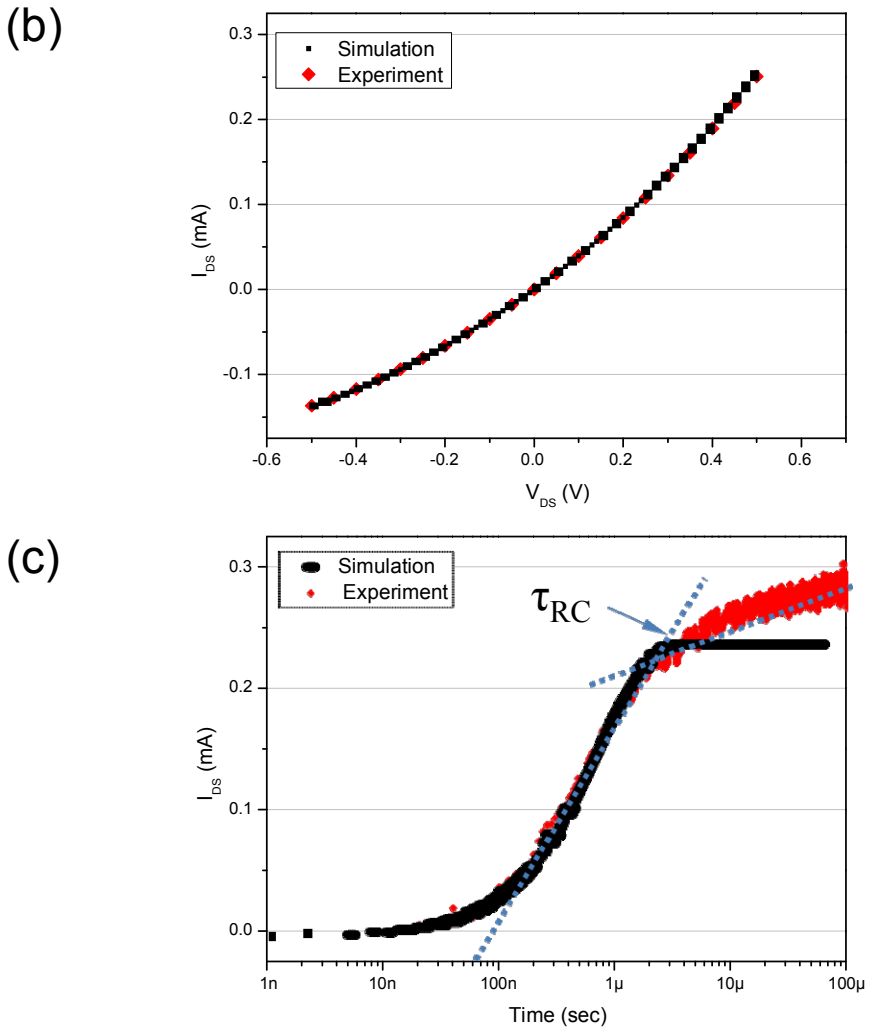


Figure S6. (a) Equivalent circuit for the CNN system in the buffer solution. (b) *I-V* characteristics of the CNN channel from simulation and measurement. (c) Transient behavior of the drain current, after the unit step of 0.5 V is applied to the drain, from simulation and measurement.

## 6. Au nanoparticle deposition method

A literature survey about the particle sizes obtained as a result of two Au deposition methods (electrochemical method, thermal evaporation method) is summarized in Table S2. From this it was observed that the average sizes, and the standard deviations of GNP by the thermal evaporation method have a similar uniformity, compared to those of results using the electrochemical method. The thermal evaporation method has a number of advantages, compared to the electrochemical method. For example, it does not require CNT surface modification, and is a single-step process with a reduced number of parameters to be controlled, and can produce large yields of uncontaminated CNT-nanoparticle composites, with good controllability of particle size (Scarselli et al., *CARBON*, 2012, **50**, 875-884).

| | **Method** | **Average Diameter (nm)** | **Standard Deviations (nm)** |
|---|---|---|---|
| Sun et al., *CARBON*, 2011, **49**, 4376-4384 | Electrochemical | 4.41 | 0.15 |
| Bhaviripudi et al., *J. Am. Chem. Soc*, 2007, **129**, 1516-1517. | Electrochemical | 3.10 | 0.40 |
| Lee et al., *CARBON*, 2005, **43**, 2654-2663. | Electrochemical | 1.66 | 0.38 |
| Scarselli et al., *CARBON*, 2012, **50**, 875-884. | Thermal evaporation | 7.90 | 0.30 |
| Our sensor platform | Thermal evaporation | 8.98 | 0.31 |

Table S2. Average diameter and standard deviation of GNP by electrochemical and thermal evaporation methods.

## 7. DNA analysis comparison

| Platform | **Limit of Detection** | **Electrolyte** | **Reference** |
|---|---|---|---|
| Layer-by-layer MWCNT-Au NP on gold electrode | 6.2 pM | STE buffer (0.05M NaCl, 0.01M Tris, 0.001M EDTA, pH 7.0) | Zhang et al., *Elctrochim. Acta,* 2009, **54**, 2385-2391 |
| Alkylated Nonoxidized Silicon Nanowires | 10 pM | 1X SSC buffer | Bunimovich et al., *J. AM. CHEM. SOC,* 2006, **128**, 16323-16331 |
| two-species hybridization reaction under ITP | 10 pM | TE (50 mM Tricine and 100 mM Bistris), LE (250 mM HCl, 500 mM Bistris, 2 mM $MgCl_2$, 0.1 % PVP) | Bercovici et al., 15th International Conference on Miniaturized Systems for Chemistry and Life Sciences, Seattle, 2011 |
| MWCNT-based multicolor Fluorescent nanobeacon for multiplexed analysis of DNA | 500 pM | 100 fold diluted serum | Chen et al., Talanta, 2013, http://dx.doi.org/10.1016/j.talanta.2013.02.003i |
| bio system composed of CNN and GNP as an electrical channel | 5 pM | Serum | This work |

Table S3. Comparison of methods for the analysis of DNA.